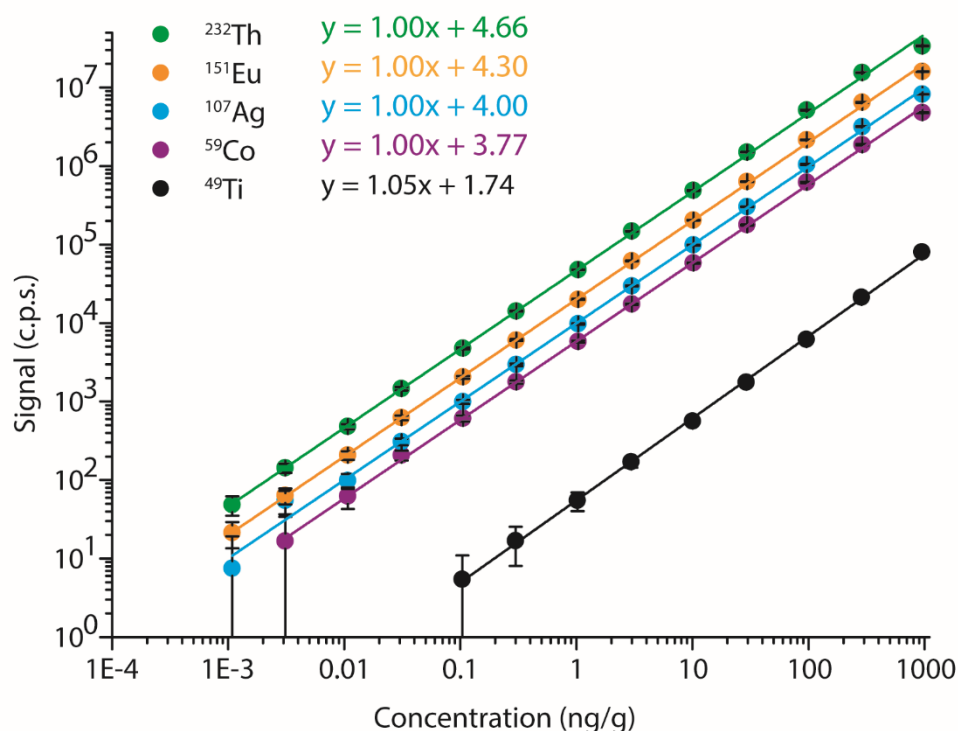


## Supplementary Information for “Characterization of a new ICP-TOFMS Instrument with Continuous and Discrete Introduction of Solutions”

Lyndsey Hendriks, Alexander Gundlach-Graham\*, Bodo Hattendorf, and Detlef Günther

*ETH Zurich, Department of Chemistry and Applied Biosciences, Laboratory of Inorganic Chemistry, Vladimir-Prelog-Weg 10, CH-8093 Zurich, Switzerland*

\* Correspondence address: [graham@inorg.chem.ethz.ch](mailto:graham@inorg.chem.ethz.ch)



**Figure S1:** Calibration curves for  $^{49}\text{Ti}$ ,  $^{59}\text{Co}$ ,  $^{107}\text{Ag}$ ,  $^{151}\text{Eu}$  and  $^{232}\text{Th}$  obtained with the conventional pneumatic nebulizer and cyclonic spray chamber sample introduction system under standard acquisition mode (i.e. covering the mass range from  $^{14}\text{N}^+$  to  $^{254}\text{UO}^+$ ). The calibration for Th spans six orders of magnitude with detection saturation occurring at  $1000\text{ ng g}^{-1}$ . The calibration curves of Co and Ti are non-linear below lowest concentration with data shown in the curve. Abundance-corrected sensitivities for all elements measured are provided in Table S2.

**Table S1:** Operating conditions for the *icp*TOF using He in the CCT and operating conditions for the *icp*TOF with focus on low mass elements (i.e. Li, Be, B).

	Collision mode	Low-mass mode
Sample Introduction Setup Description	Pneumatic nebulizer with cooled cyclonic spray chamber	Pneumatic nebulizer with cooled cyclonic spray chamber
Plasma Power [W]	1550	1600
Central Gas Flow [l/min]	1.1	1.1
Auxiliary Gas Flow [l/min]	0.8	0.8
Cooling Gas Flow [l/min]	17	17
Sampling Depth [mm]	5	5
Injector Diameter [mm]	2	2
Collision Cell Gas [V]	3 mL/min He	No gas
CCT Amplitude [V]	250	80
CCT Bias [V]	1	-6
Notch Amplitude [V]	250	120
Notch Bias	-16	-50
Masses Notched	$^{16}\text{O}^+$ , $^{14}\text{N}_2^+$ , $^{16}\text{O}_2^+$ ,	$^{16}\text{O}^+$ , $^{14}\text{N}_2^+$ , $^{16}\text{O}_2^+$ , $^{40}\text{Ar}^+$
TOF Repetition Rate	33 kHz	33 kHz
Detected Mass Range	14 – 275 m/z	7– 175 m/z*
(CeO/Ce)**	<2.3%	<1.3%
Data Acquisition	continuous mode	continuous mode
TOF Time Resolution	300 ms	300 ms

**Table S2:** Overview of the sensitivities, concentration LODs, and absolute LODs achieved with both sample introduction systems, as well as for ensemble averaging of droplets. Measurements were done in the standard *icp*TOF operation mode (i.e. no gas in the collision/reaction cell and covering a mass range from  $^{14}\text{N}$  to  $^{254}\text{UO}^+$ ).

Elements	PN			1 droplet		1000 droplets summed	
	Abundance-corrected sensitivities	LOD concentration	LOD absolute mass	LOD concentration	LOD absolute mass	LOD concentration	LOD absolute mass
	cps/[ng g <sup>-1</sup> ]	ng g <sup>-1</sup>	fg	ng g <sup>-1</sup>	ag	ng g <sup>-1</sup>	ag
Li	N/A	N/A	N/A	N/A	N/A	N/A	N/A
Mg	1970	0.1	27	930	9000	3	31970
Al	2100	0.1	20	340	3100	2	20600
Ti	1520	0.2	47	140	1300	1	8164
Co	6430	0.01	4	8	74	0.1	1055
Y	20950	0.001	0.2	2	17	0.01	126
Ag	21490	0.003	0.8	6	56	0.03	244
In	24960	0.001	0.3	2	17	0.009	88
Cs	23690	0.001	0.4	3	25	0.06	596
La	30160	0.002	0.5	1	10	0.004	35
Ce	34480	0.002	0.4	1	13	0.005	46
Eu	48630	0.0003	0.07	2	18	0.03	249
Lu	56590	0.0001	0.02	0.6	6	0.003	25
Pb	52590	0.003	0.8	1	13	0.006	58
Bi	43060	0.0004	0.09	0.9	9	0.004	42
Th	53950	0.0001	0.03	0.6	6	0.002	22
U	58770	0.0002	0.04	0.6	5	0.002	18

**Table S3:** Overview of the sensitivities and concentration LODs achieved with He as collision gas in the CCT.

	<b>Abundance Corrected Sensitivity cps/[ng g<sup>-1</sup>]</b>	<b>LOD pg g<sup>-1</sup></b>
Li	N/A.	N/A
Mg	160	412
Al	140	1251
Ti	1140	316
Co	3470	16
Y	7890	1
Ag	14100	3
In	16320	1
Cs	17500	1
La	21510	1
Ce	27040	0.7
Eu	47000	1
Lu	60500	0.2
Pb	66820	5
Bi	53480	0.6
Th	62380	0.2
U	84400	0.2

**Table S4:** Overview of the sensitivities and concentration LODs recorded using the low-mass tune settings.

	<b>Abundance Corrected Sensitivity cps/[ng g<sup>-1</sup>]</b>	<b>LOD ng g<sup>-1</sup></b>
Li	900	0.05
Be	100	0.06
B	210	1
Mg	2730	0.2
Al	1770	0.07
Ti	180	2
Co	1170	0.02
Y	970	0.01
Ag	110	0.1
In	70	0.1
Cs	10	0.7
La	5	1
Ce	5	2
Eu	2	7
Lu	0.2	30
Pb	0.03	440
Bi	0.02	290
Th	0.01	560
U	0.01	420

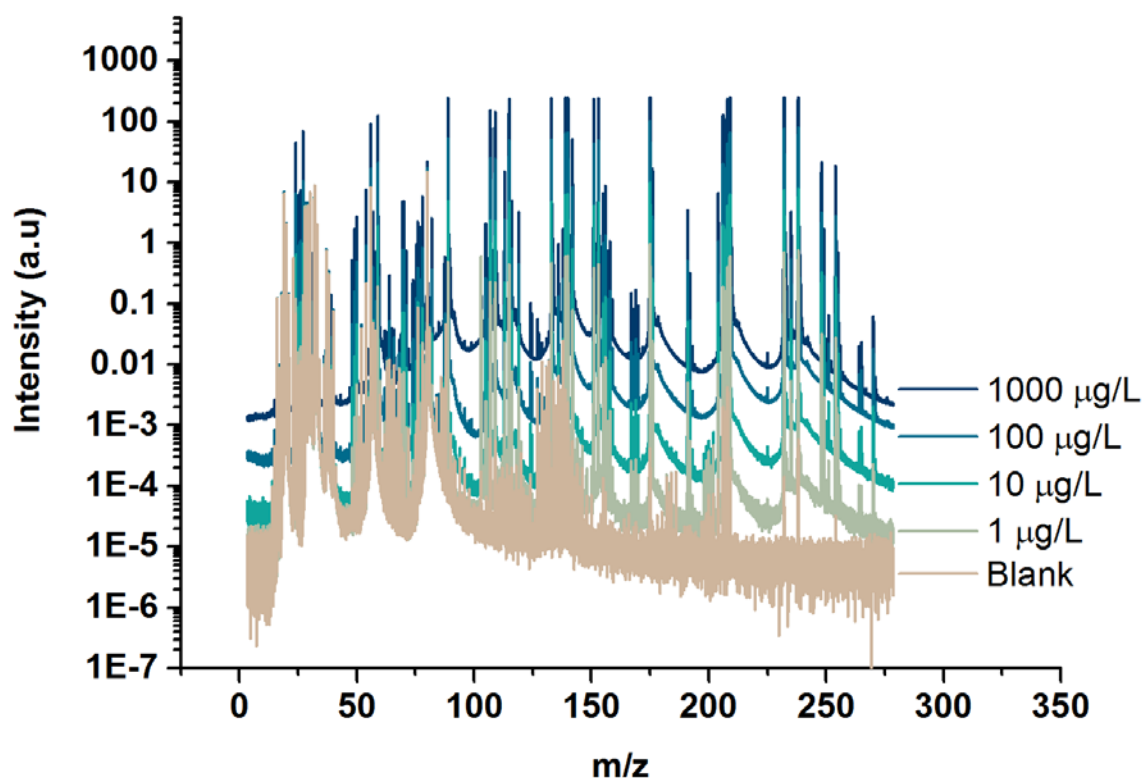


**Figure S2.** Complete mass spectra from the multi-element calibration obtained with a pneumatic nebulizer as introduction system show dramatic increases in baseline with concentrations. From the blank mass spectrum to the spectrum from the 1000 ng/g multi-element solution, the baseline increases from two to three orders of magnitude. Elevated baseline is caused by stray ions and scattered ions from ions introduced into the TOF mass analyzer and the effects are largest on the high- $m/z$  side (longer flight time) of major peaks. The baseline elevation at the high- $m/z$  region of the mass spectrum is greater than that at the low- $m/z$  region because the peak tails and stray-ion envelopes build up on the high- $m/z$  side. As discussed in the main text, the effects of baseline elevation can be mostly eliminated through fitting and subtraction of the baseline.

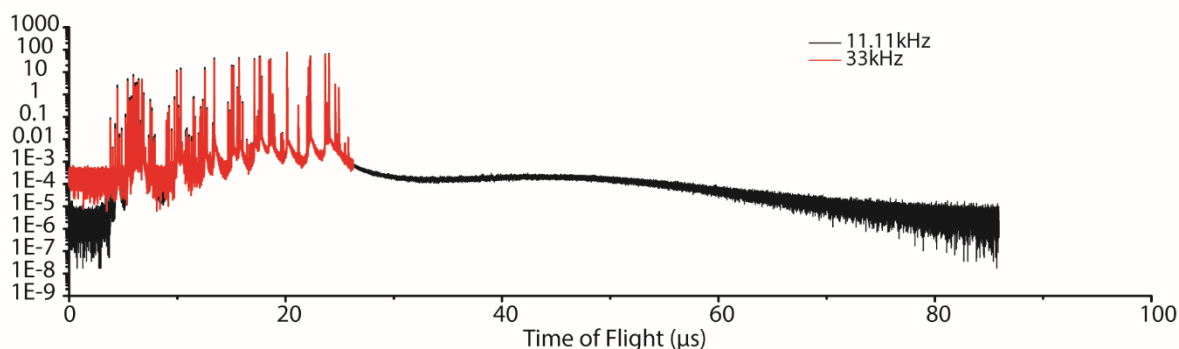


**Figure S1:** To better understand the source of baseline elevation in the *icp*TOF, the 100 ng g<sup>-1</sup> multi-elemental solution was recorded with the standard total flight time of 30 μs (33 kHz TOF repetition rate) and an extended TOF window of 90 μs (11.11 kHz TOF repetition rate). In the standard TOF acquisition mode (red trace), the baseline is elevated exactly as shown in Figure S2, with elevated baseline across the entire mass spectrum (now shown in time-of-flight rather than calibrated into *m/z* values). In the extended flight time TOF acquisition mode, we observe that the elevated baseline apparent in the normal TOF measurement window extends well beyond the 30 μs it takes for atomic ions to be mass separated in the flight tube. As seen, the baseline does not return to background levels until about 50 μs after the end of TOF mass separation period, i.e. until about 80 μs after TOF extraction. These stray ions do not have clear energy or *m/z*-dependent flight times and so do not reach the detector as discrete packets, but rather as a continuous baseline signal. The “washout” time of background ions indicates that the baseline is characterized by stray and scattered ions that are initially present in the ion packet at the onset of the TOF extraction and are pushed into the flight region at the same time as the ions that make up the well-defined TOFMS peaks. In fact, the “washout” of stray ions from the TOF mass analysis chamber is long enough that, in a standard TOFMS experiment with a 33-kHz repetition rate, stray ions from up to two previous TOFMS extractions are present when a TOF mass spectrum is measured. This wrap-around effect of stray ions in the TOFMS is apparent when the 30-μs and 90-μs mass spectra are compared. In the 90-μs spectrum, the baseline at the beginning of the TOF analysis has returned to the true instrument background level. However, the 30-μs spectrum shows elevated baseline from the beginning of the TOF analysis and the magnitude of this background elevation matches the magnitude of elevated background visible just after the end of the standard TOF analysis, i.e. at the *start* of the next TOF analysis. In the 90-μs spectrum, some long range structure to the baseline is apparent as a broad peak around a flight time of 50 μs; we are currently investigating the cause of this structured baseline.

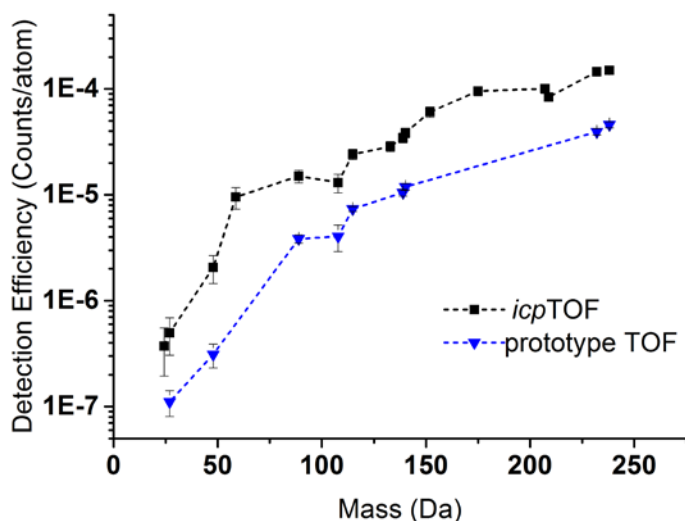


**Figure S4.** Comparison of the detection efficiencies achieved between the prototype ICP-TOFMS instrument and the new, commercially available *icp*TOF using microdroplet generation (MDG) sample introduction. Different solutions were measured with the two instruments, though many elements are common in both. Lines connecting the data points are drawn to help guide the eye, but are not supported by data. Error bars on the y-axis were computed from the standard deviation of the signal intensity of ~2500 droplets.